





## The Toba supervolcano eruption caused severe tropical stratospheric ozone depletion

Sergey Osipov <sup>1</sup>✉, Georgiy Stenchikov <sup>2</sup>, Kostas Tsigaridis <sup>3,4</sup>, Allegra N. LeGrande<sup>3,4</sup>, Susanne E. Bauer<sup>4</sup>, Mohammed Fnais<sup>5</sup> & Jos Lelieveld <sup>1</sup>

Supervolcano eruptions have occurred throughout Earth's history and have major environmental impacts. These impacts are mostly associated with the attenuation of visible sunlight by stratospheric sulfate aerosols, which causes cooling and deceleration of the water cycle. Supereruptions have been assumed to cause so-called volcanic winters that act as primary evolutionary factors through ecosystem disruption and famine, however, winter conditions alone may not be sufficient to cause such disruption. Here we use Earth system model simulations to show that stratospheric sulfur emissions from the Toba supereruption 74,000 years ago caused severe stratospheric ozone loss through a radiation attenuation mechanism that only moderately depends on the emission magnitude. The Toba plume strongly inhibited oxygen photolysis, suppressing ozone formation in the tropics, where exceptionally depleted ozone conditions persisted for over a year. This effect, when combined with volcanic winter in the extra-tropics, can account for the impacts of supereruptions on ecosystems and humanity.

<sup>1</sup>Max Planck Institute for Chemistry, Mainz, Germany. <sup>2</sup>King Abdullah University of Science and Technology, Thuwal, Saudi Arabia. <sup>3</sup>Columbia University, New York, NY, USA. <sup>4</sup>NASA Goddard Institute for Space Studies, New York, NY, USA. <sup>5</sup>King Saud University, Riyadh, Saudi Arabia. ✉email: [Sergey.Osipov@mpic.de](mailto:Sergey.Osipov@mpic.de)

Throughout Earth's history volcanic eruptions have perturbed the climate and caused regional and global environmental disasters, notably by creating a sunlight reflecting aerosol layer in the stratosphere that can persist for many years. In 1991 the Mount Pinatubo eruption in the Philippines released nearly 20 Mt of sulfur dioxide (SO<sub>2</sub>) into the stratosphere which oxidized into sulfate aerosols, which then caused a global cooling of the oceans of about 0.3 °C and prolonged an El Niño event<sup>1–4</sup>. In 1815 the Tambora eruption in Indonesia injected three times more SO<sub>2</sub> into the stratosphere, which produced 0.7 °C global cooling, with profound environmental impacts, including the “year without a summer” in 1816<sup>5–7</sup>. Following the Tambora eruption, anomalous cooling and reduced precipitation provoked crop failure, famine, and the outbreak of diseases such as cholera in North America, Europe and Asia. The Toba supervolcano eruption at 74 ka has been the largest natural disaster known in the past 2.5 million years<sup>8</sup>. It injected up to 100 times more SO<sub>2</sub> into the stratosphere than Mt Pinatubo, and climate model simulations suggest a global cooling of 3.5–9 °C, and up to 25% reduction in precipitation<sup>9–12</sup>. Due to the scale and magnitude of such volcanic winter effects, several supereruptions have had a distinct footprint in planetary history, and need to be accounted for in theories of human evolution, notably of *Homo sapiens* in the past 200 ka.

The volcanic winter concept was consolidated after it was implicated as an important evolutionary factor, often linked to the Toba eruption. A common theory of the origin and dispersal of modern humans suggests that *Homo sapiens* spread from a single tropical African source, though experienced dramatic reduction in effective population size down to 1000–10,000 individuals<sup>13,14</sup>. According to DNA analysis, a population bottleneck happened around 50–100 ka<sup>15,16</sup>, during the peak of the glacial stage ( $\delta^{18}\text{O}$  5a-4), after climate transitioned from a relatively warm to a cold state, i.e., during glaciation. Based on the coincidence of these two factors with the supervolcano eruption, the Toba catastrophe theory was put forward to explain the human genetic bottleneck as well as the onset of the glacial period<sup>13,14</sup>.

Recently, the Toba catastrophe hypothesis has become disputed and the paleoanthropological support has dwindled notably from progress in genomics, improved climate modeling, and new paleoenvironmental core samples from eastern Africa. With the advancement of whole-genome sequencing, the possible bottlenecks are now dated around 50 ka<sup>15,17</sup> and 130–150 ka<sup>18</sup> and could also be explained via the founder effect (small size of the founding population)<sup>19</sup> in addition to a population reduction. While these studies and the lack of consensus between genomics interpretations do not exclude the bottleneck around the Toba event horizon, none of the wide range of dates pinpoints the bottleneck exactly to the Toba eruption at 74 ka.

The petrological estimates of the sulfur emissions from the Toba eruption is another line of argumentation that has questioned the catastrophe theory. Analyses based on the melt inclusion technique suggested that the Toba eruption was anomalously sulfur-poor (as low as 3–6× Pinatubo), while being extremely halogen-rich at the same time (as high as 300× the average Central American Volcanic Arc eruption, considered to be particularly halogen-rich)<sup>20–22</sup>. This low, controversial estimate of the sulfur emissions, which implies a non-catastrophic magnitude of the volcanic winter, is not Toba specific but is a part of an emerging “sulfur paradox”. For almost all volcanic eruptions during the satellite era, the petrologic indicators and sulfur yield in magma predict SO<sub>2</sub> emissions at least 1 order of magnitude smaller than measured using remote sensing methods<sup>23,24</sup>. The discrepancy between petrologic and remote sensing estimates is probably due to the presence of an exsolved vapor phase in the

magma before eruption<sup>23,25,26</sup> and petrologic estimates therefore underestimate the total erupted sulfur amount. While the “missing” sulfur source remains to be better understood and quantified to resolve this paradox, a sulfur-rich supereruption around the Toba event horizon (up to 100× Pinatubo) is evident from multiple climate proxies: the analyses of ice cores from both hemispheres<sup>27,28</sup> and the integral ocean cooling from studies of coral reefs<sup>29,30</sup>.

Paleoclimatic reconstructions from Lake Malawi sediments in tropical Africa and the simulated magnitude of the volcanic winter climate perturbations are the least conflicting among arguments that discredit the Toba catastrophe theory. Climate model simulations do not corroborate the initiation of glaciation<sup>10,31</sup>, but substantiate the global extent of strong climate cooling. The recent global climate simulations with improved representation of stratospheric chemistry and aerosol microphysics mechanisms have shown that the volcanic winter effects are significantly less extreme than assumed originally<sup>11,12,32</sup>. The new simulations suggest that the global mean cooling could peak at 3.5 °C (rather than 15 °C, assumed previously) and that the sulfate aerosol optical depth (which causes the radiative forcing of climate) returns to background levels within 4–5 years (rather than 20 years). This magnitude of the simulated surface cooling represents the lower limit of many model studies, which is in line with the recent analyses of the lake Malawi sediments. The sediment core analysis, although with a resolution of 9 years per record, substantiate reduced precipitation and consequent vegetation perturbation after the Toba eruption, but do not confirm a cooling event that could have been catastrophic for humans<sup>19,33</sup>.

Here we present a complementary, solar ultraviolet (UV) radiation volcanic catastrophe theory, which highlights that the volcanic impact is represented by a spectrum of environmental stresses rather than by climate cooling and drying only. We show that the Toba volcanic plume caused massive ozone (O<sub>3</sub>) loss and produced hostile UV radiation conditions at the Earth's surface, particularly in the tropics. To account for uncertainties, we cover the range of sulfur emissions (1–100× Pinatubo) to illustrate that these environmental and evolutionary stress factors are general and do not strongly depend upon the magnitude of the model simulated or sediment-analyzed volcanic winter effects.

## Results

In view of the fundamental life-protecting role of stratospheric ozone on our planet, several environmental disaster options and catastrophic ozone loss mechanisms have been considered. For example, in a nuclear winter scenario smoke and soil particles from explosions and fires are expected to reach the stratosphere, leading to local heating from the absorption of sunlight (by black carbon) and cooling the Earth's surface<sup>34,35</sup>. The stratospheric heating allows more water vapor to cross the tropical tropopause, which accelerates catalytic ozone loss by hydrogen and nitrogen containing species<sup>35</sup>. Catalytic ozone loss by anthropogenic halogen (chlorine and bromine) compounds has been identified as the cause of stratospheric ozone depletion in the past half century, resulting in the recurrent exceptionally depleted ozone conditions over Antarctica during austral spring, when column O<sub>3</sub> drops below 220 Dobson Units (DU), reaching minima below 125 DU<sup>36</sup>. The catastrophic ozone loss over Antarctica results from the heterogeneous chemical interactions between halogens and polar stratospheric clouds that form in this extremely cold part of the stratosphere. Such chemistry also takes place on sulfate particles, and large volcanic eruptions that inject both sulfur and halogen species are expected to contribute to ozone loss<sup>21,37,38</sup>. The halogen loading from volcano eruptions can vary greatly depending on the composition of the magma. For example, Mt

Pinatubo did not release much halogen containing compounds into the stratosphere, whereas large explosive eruptions in Central America, such as that of Los Chocoyos at about 81 ka, may have led to exceptionally depleted ozone conditions, characterized by a column abundance less than 220 DU<sup>21,22</sup>.

Here, we consider an additional volcanic and radiation attenuation mechanism that influences ozone and surface UV radiation. Chemical ozone production is highest in the lower tropical stratosphere, from the photolysis of oxygen by solar photons with a wavelength  $\lambda < 242$  nm, because at low latitudes shortwave solar radiation is particularly intense. During volcanically quiescent conditions, absorption by O<sub>3</sub> and molecular Rayleigh scattering control radiative transfer at these wavelengths. But massive tropical volcanic eruptions such as that of Toba give rise to large amounts of SO<sub>2</sub> and sulfate aerosols in the stratosphere, which strongly enhance the UV extinction optical depth. The SO<sub>2</sub> cloud strongly absorbs UV radiation, and weakly absorbing sulfate additionally scatters the photons back to space, which decreases the radiation flux needed to form ozone within and below the volcanic plume<sup>39,40</sup>. We computed the Toba effects on solar photon fluxes with a detailed radiative-transfer model, showing shutdown of the O<sub>2</sub> photolysis and a strong reduction of O<sub>3</sub> within the volcanic plume<sup>39</sup> (“Methods”). Since the spectral absorption of SO<sub>2</sub> overlaps with that of O<sub>3</sub>, both the photochemical sources and sinks of ozone are perturbed under these conditions, which moreover delays the conversion of SO<sub>2</sub> into sulfate, sustaining the plume lifetime but reducing the climate impact in the tropics<sup>12,41,42</sup>.

To quantify the combined radiative, chemical, and circulation impacts of the Toba eruption, we applied the NASA-GISS ModelE global interactive atmospheric chemistry-climate model, assuming an SO<sub>2</sub> injection into the stratosphere of about 100 times that of Mt Pinatubo (“Methods”). Our simulations indicate massive ozone depletion that peaks at about 20% globally in half a year, and recovery to near-background levels in three years. This anomaly was most devastating at low latitudes where column ozone declined by more than a factor of two, from >250 to <125 DU (Fig. 1). In the Methods section we present sensitivity calculations of SO<sub>2</sub> injections that are up to orders of magnitude smaller, showing that the impact is not strongly dependent on the size of the eruption. With a 20-times Pinatubo simulation, we still find a tropical ozone depletion that is more severe and much larger than the current one over Antarctica, with a duration of nearly a year, and a column O<sub>3</sub> minimum below 175 DU for several months. Subsequent to the Toba perturbation of the tropical stratosphere, advection by the large-scale overturning (Brewer–Dobson) circulation redistributed the plume toward the extra-tropics, which reduced UV radiation penetration to the surface at those latitudes, but enhanced it in the tropics (Fig. 2). Figure 2 shows that the aerosol optical depth (AOD, being the sunlight extinction) maximized outside the tropics, especially in the Northern Hemisphere where the Brewer–Dobson circulation is strongest. Therefore, volcanic winter conditions were most severe poleward of 20° latitude, consistent with the Lake Malawi sedimentary data analyses that indicate only limited cooling in the tropics<sup>19,33</sup>.

Conditions 6–12 months after the eruption roughly represent the apogee of the Toba environmental impacts, i.e., in terms of UV exposure and cooling at the surface. At this stage of the volcanic plume evolution the SO<sub>2</sub> was mostly converted into sulfate, and the aerosol optical depth at middle latitudes reached a maximum of >5 (Fig. 2, Fig. 3 and “Methods”). This means that only a small fraction of the sunlight could penetrate the plume for about a year during the already cold glacial climate. Furthermore, tropical stratospheric ozone had collapsed. Our calculations indicate that near the equator O<sub>3</sub> declined to 125 DU, which

translates into a 140% increase of the maximum daily UV index (UVI) from a background value of about 12 to about 28 (“Methods”). A UV index larger than 10 is already considered “extreme” by the World Health Organization (WHO) in terms of the need for protection, and causes sunburn damage in about 15 min. Nevertheless, the surface UVI increase due to ozone loss was partially mitigated by the volcanic plume itself. During the initial stage of the eruption, 2000 Mt of emitted SO<sub>2</sub> (comparable to the global O<sub>3</sub> inventory of 3200 Mt) or 350 DU in tropics, almost entirely blocked UV radiation. Afterward, during the peak AOD stage of the volcanic plume evolution, SO<sub>2</sub> was converted into the less efficiently UV-absorbing sulfate aerosols, leading to a partial offset of the ozone depletion and the associated UVI increase. This explains the non-linear behavior as a function of plume size, and the moderate dependence upon the assumed amount of SO<sub>2</sub> emitted by the Toba eruption.

The high tropical UV index was perpetuated for about a year, because the gradual weakening of the ozone depletion was counteracted by waning aerosol shielding. At middle latitudes the ozone loading was reduced but did not drop below 275 DU, being close to the climatological value at the equator, while the volcanic plume inhibited UV radiation transmission. It thus appears that the Toba climate and UV impacts were distributed meridionally and acted complementary. The tropics were most strongly affected by highly detrimental UV levels, in part related to the low solar zenith angles, while volcanic winter (cooling and drying), with an intensity much beyond that of Tambora in 1816, caused extreme weather conditions at extra-tropical latitudes.

## Discussion

The UV index increase (i.e., several times above the maximum on the WHO scale) over a period of about a year is likely to have had critical consequences for humanity, although biomedical studies of such conditions are not available to test the specific outcomes. The range of possible UV impacts is extensive, with environmental, ecological, health-hazardous and societal consequences<sup>43</sup>. In the short term, health risks include eye damage (photokeratitis and photoconjunctivitis) and erythema. Hindered vision (painful inflammatory reactions) and sunburns combined with the decay of precipitation and shortfall of food availability must have significantly worsened survival challenges. In the longer term, the increased carcinogenesis (cataract and skin cancer), immune system suppression, and general DNA damage<sup>44</sup> likely added to a potential population decline. Overall, the magnitude of UV-induced health-hazardous effects following the Toba super-eruption were more severe and much longer lasting than those during the recent exceptionally depleted ozone conditions, located over populated land (contrary to Antarctica), including most of Africa, and several times larger than during the aftermath of a massive hypothetical nuclear conflict<sup>34,35</sup>.

Although it remains difficult to quantitatively determine the environmental impacts of a supervolcano eruption at 74 ka, it is unlikely that we have underrated the role of a tropical stratospheric ozone depletion. The physical mechanism of radiation extinction and O<sub>3</sub> formation is straightforward, and even with a much-reduced amount of stratospheric aerosol our results are robust. Furthermore, we have not included the chemical impact of halogen compounds, which catalytically destroy ozone, as there is no reliable information on their emissions from Toba. While the indications that the Toba eruption was halogen-rich are weak, some fraction of these compounds will have been co-emitted and will have aggravated ozone loss<sup>22</sup>, hence our results represent a lower limit of the UV increase. For example, we can compare the Toba eruption with that of Krakatau in Indonesia, with Toba injecting orders of magnitude more SO<sub>2</sub> into the stratosphere,

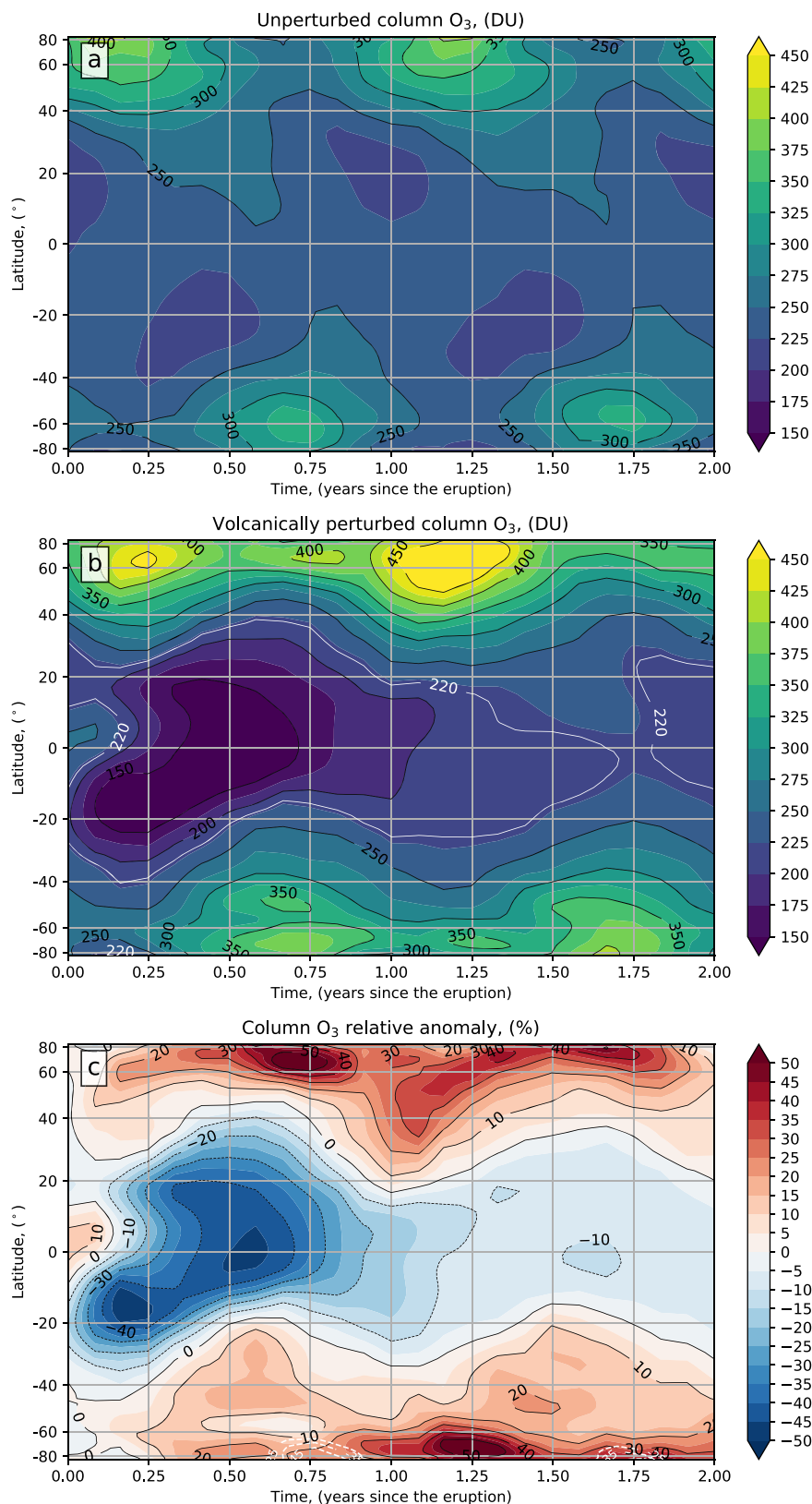


**Fig. 1 Model calculated zonal mean column ozone.** **a** Volcanically unperturbed column ozone. **b** Effect of the Toba eruption. The white 220 DU contour line highlights the area according to the definition of the modern-day exceptionally depleted ozone conditions. **c** Volcanically induced relative change. The white dashed contour lines in **c** highlight the extent of the modern-day exceptionally depleted ozone conditions over Antarctica, which peaks in late September–October. These data from atmospheric reanalyses<sup>58</sup> span the years 2015–2016 and represent one of the strongest ozone depletion events on record. The white dashed contour lines are computed with respect to 300 DU, starting at 25% and maximizing at 60%. The model is GISS ModelE<sup>49</sup>.

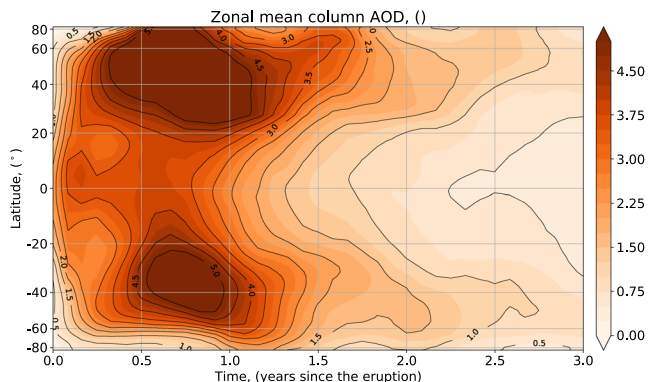


**Fig. 2 Model calculated zonal mean aerosol optical depth.** Aerosol optical depth at visible wavelengths after the Toba eruption. Note that the extent of the hemispheric asymmetry depends on the time of year of the eruption, which is not known.

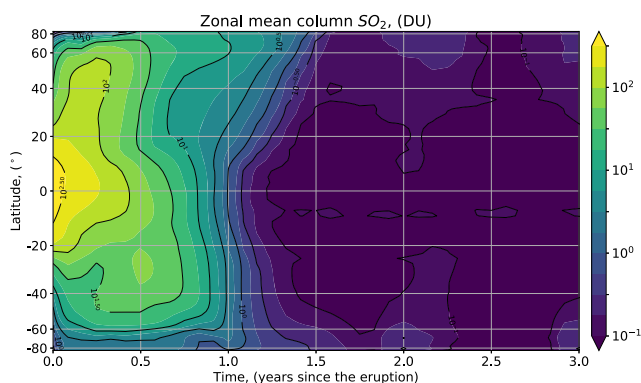


**Fig. 3 Model calculated zonal mean column SO<sub>2</sub>.** Column SO<sub>2</sub> after the Toba eruption. Note the logarithmic scale.

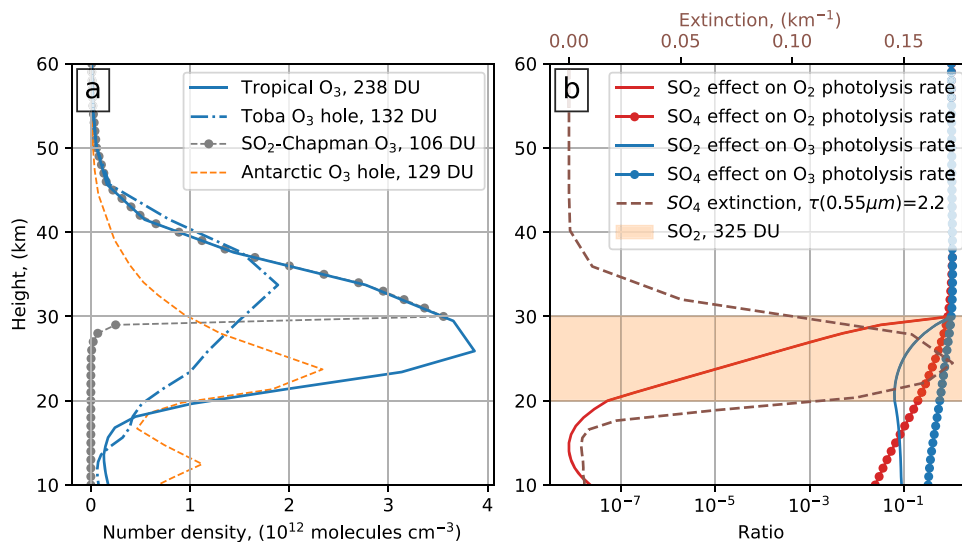


**Fig. 4 Radiative effects of the Toba volcanic plume on the photolytic sources and sinks of ozone.** The radiative effects of the Toba volcanic plume are computed for the equatorial atmosphere using a tropospheric ultraviolet and visible (TUV) radiative transfer model. **a** Various vertical profiles of ozone: unperturbed tropical profile; tropical ozone depletion 6 months after Toba eruption; profile predicted by the Chapman equation of ozone chemistry and SO<sub>2</sub> effects; and the recent Antarctic ozone depletion. **b** Ratio of the volcanically perturbed and unperturbed photolysis rates (daytime mean) of O<sub>2</sub> and O<sub>3</sub> due to volcanic plume presence (SO<sub>2</sub> and SO<sub>4</sub>). Shaded area between 20 and 30 km represents initial SO<sub>2</sub> cloud. The SO<sub>4</sub> profile is 1 month old. The SO<sub>2</sub>-Chapman ozone profile is derived by scaling the unperturbed ozone profile. The scaling weights are derived from the Chapman equation and photolysis rate ratios shown in **b**.

while chlorine emissions from Krakatau may have caused about 7% of column ozone depletion<sup>22</sup>. Considering the scale of these impacts, it seems likely that halogen-induced chemistry from Toba has added substantially to the depth of the tropical ozone decline.

Our proposed stratospheric ozone and UV calamity extends the concept of the volcanic winter effects and offers a way to reconcile the seemingly conflicting data about classical volcanic winter conditions, which, for example, have been shown to be insufficiently severe in Africa to bring humanity to the verge of extinction<sup>19,33</sup>. The radiation attenuation mechanism from volcanic sulfur emissions, inherent to any volcanic eruption, presents a plausible ozone-UV scenario. We note the role of volcanic halogens, which enhance the ozone loss<sup>21,45,46</sup> in addition to the radiation mechanism proposed here.

In a broader view, the ozone-UV scenario augments the classical volcanic winter theory. For example, our findings are in line with and complement the emerging evolutionary role of stratospheric ozone across the much wider time scales extending to the end-Permian crisis<sup>47,48</sup>. We conclude that limited cooling and drying plus severe biological UV damage in the tropics, combined with harsh volcanic winter conditions in the extra-tropics, could have provided the prerequisites for a population bottleneck. Finally, we recommend that the impact of sunlight extinction by thick stratospheric aerosol plumes on ozone formation are accounted for in future studies of the environmental consequences of explosive volcanoes, nuclear conflicts, and solar radiation management (geoengineering).

**Methods**

**Model setup and experiments.** We analyzed the volcanic plume evolution and impacts on atmospheric chemistry using the Goddard Institute for Space Studies (GISS) Earth system model (ModelE) simulations. Below we highlight the details specific to this study, while ref. 49 provides a complete description of ModelE and ref. 12 describes the model setup and simulations.

To simulate the volcanic plume evolution, ModelE includes fully interactive chemistry related to ozone<sup>50</sup> and sulfate<sup>51,52</sup>. The eruption of Toba is modeled by the instantaneous injection of 2000 Mt of SO<sub>2</sub> (about 100× Pinatubo<sup>53</sup>) at the

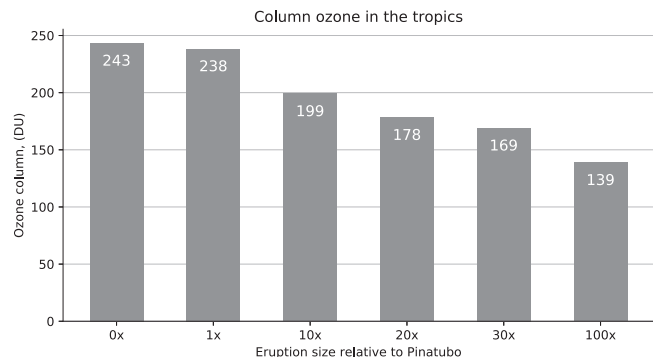


**Fig. 5 Tropical ozone column as a function of volcanic eruption size in multiples of that of Pinatubo.** Note that the simulated atmosphere represents paleoclimatic conditions at 74 ka and does not include anthropogenic halogens. The observed post-Pinatubo ozone depletion in 1991 was stronger than presented here due to heterogeneous chemical processing of anthropogenic halogen species<sup>45</sup>.

beginning of the year. Emitted SO<sub>2</sub> is distributed with a mixing ratio of about 11 ppmv in the 20S–20N equatorial belt between 10 and 50 hPa.

**Photochemistry and effects of SO<sub>2</sub> and microphysics.** Actinic fluxes and photolysis rates were calculated in the presence of cloud and aerosol layers, using the accurate and efficient Fast-J2 scheme<sup>54,55</sup>. However the original scheme was not designed to capture the effects of volcanic plumes on stratospheric ozone chemistry, and several essential improvements were implemented. Here the full multiple-scattering code was used to compute the radiation field above wavelengths of 200 nm (previously 291 nm, important for O<sub>2</sub> photolysis), which replaces the default pseudo-absorption simplification<sup>55</sup>. Figure 4 shows the radiative effects of the volcanic plume on O<sub>2</sub> and O<sub>3</sub> photolysis, computed with the reference model (Tropospheric Ultraviolet and Visible radiation model<sup>56</sup>). SO<sub>2</sub> strongly absorbs in the UV part of the spectrum (similar to O<sub>3</sub>) and inhibits photolytic ozone loss<sup>12</sup>. Along with aerosols, SO<sub>2</sub> was coupled to the photochemistry, and its radiative effects at UV wavelengths were taken into account.

We also incorporated the microphysics of the aerosols and their effects on the spectral optical properties on ozone photochemistry. Coagulation and growth of the sulfate aerosol droplets decreases the extinction efficiency per unit mass for shorter wavelengths. In the visible spectrum, this effect reduces the efficiency of radiative cooling by volcanic aerosols and modulates climate impact. Similarly, we coupled the dependence of aerosol extinction in the UV on the size distribution into the Fast-J2 code. The microphysics, particle growth, and UV scattering efficiency control the volcanic impact on stratospheric ozone. Figure 5 shows that the ozone loss non-linearly reduces with the size of the eruption, indicating that the depth of the tropical ozone depletion does not strongly depend on assumptions about the eruption magnitude.

**UV index.** We define the UV index (UVI) as

$$\text{UVI} = \frac{11}{17.25} \frac{1}{\text{mWm}^{-2}} \int_{286.5 \text{ nm}}^{400 \text{ nm}} I(\lambda) w(\lambda) d\lambda \quad (1)$$

where  $I(\lambda)$  is the spectral actinic flux and  $w(\lambda)$  is the erythemal weighting function<sup>57</sup>.

In addition to ozone, optical properties of the SO<sub>2</sub> and sulfate aerosols should be taken into account to capture the perturbations of the surface UV radiation. The concentrations of these radiative agents and their effects on UV radiation evolve in time. During the initial stage of volcanic plume evolution, the still unperturbed ozone column and maximum SO<sub>2</sub> concentrations almost entirely block the UV radiation, preventing it from reaching the surface. The suppression the O<sub>2</sub> photolysis is strongest, but O<sub>3</sub> depletion is not instantaneous and equilibration takes time. As the volcanic plume evolves, the surface UVI near the equator increases due to depletion of the ozone (Fig. 1) and SO<sub>2</sub> columns (Fig. 3, note the log scale) as it is oxidized into SO<sub>4</sub>. Approximately 9 months after the eruption, SO<sub>2</sub> is almost entirely oxidized (10 DU compared to the initial 350 DU), and O<sub>3</sub> column depletion peaks around 40–45% (DU). The effective radius of sulfate aerosols also maximizes after 9 months, reducing the efficiency to scatter the UV radiation. The enhanced SO<sub>4</sub> loading partially offsets the increased UVI due to ozone depletion. Together, perturbed O<sub>3</sub>, SO<sub>2</sub>, and SO<sub>4</sub> combine to produce the largest overall increase in UVI near the equator after about 9 months. During the final stage of the volcanic plume evolution, the surface UVI returns to the background level as SO<sub>4</sub> is removed from the atmosphere and O<sub>3</sub> recovers.

## Data availability

The simulations data are publicly available through KAUST Repository <http://hdl.handle.net/10754/667404>.

## Code availability

The ModelE model is developed by the NASA-GISS, and the radiative transfer TUV model is developed by the National Center for Atmospheric Research (NCAR). Both models are publicly available. The snapshot of the ModelE source code used in this study is archived at [https://github.com/SeregaOsipov/NASA-GISS-ModelE/releases/tag/toba\\_o3](https://github.com/SeregaOsipov/NASA-GISS-ModelE/releases/tag/toba_o3). The newly developed features will be merged into the next model version and available through the official source at <https://simplex.giss.nasa.gov/snapshots/>.

Received: 22 October 2020; Accepted: 4 March 2021;

Published online: 12 April 2021

## References

- McCormick, M. P., Thomason, L. W. & Trepte, C. R. Atmospheric effects of the Mt Pinatubo eruption. *Nature* **373**, 399–404 (1995).
- Robock, A. Volcanic eruptions and climate. *Rev. Geophys.* **38**, 191–219 (2000).
- Stenchikov, G. L. et al. Radiative forcing from the 1991 Mount Pinatubo volcanic eruption. *J. Geophys. Res. Atmos.* **103**, 13837–13857 (1998).
- Preddybaylo, E., Stenchikov, G. L., Wittenberg, A. T. & Zeng, F. Impacts of a Pinatubo-size volcanic eruption on ENSO. *J. Geophys. Res. Atmos.* **122**, 925–947 (2017).
- Stothers, R. B. The Great Tambora eruption in 1815 and its aftermath. *Science* **224**, 1191–1198 (1984).
- Luterbacher, J. & Pfister, C. The year without a summer. *Nat. Geosci.* **8**, 246–248 (2015).
- Stenchikov, G. et al. Volcanic signals in oceans. *J. Geophys. Res. Atmos.* **114** <https://doi.org/10.1029/2008JD011673> (2009).
- Chesner, C. A., Rose, W. I., Deino, A., Drake, R. & Westgate, J. A. Eruptive history of Earth's largest Quaternary caldera (Toba, Indonesia) clarified. *Geology* **19**, 200–203 (1991).
- Rampino, M. R. & Self, S. Volcanic winter and accelerated glaciation following the Toba super-eruption. *Nature* **359**, 50 (1992).
- Robock, A. et al. Did the Toba volcanic eruption of 74 ka B.P. produce widespread glaciation? *J. Geophys. Res. Atmos.* **114** <https://doi.org/10.1029/2008JD011652> (2009).
- Timmreck, C. et al. Aerosol size confines climate response to volcanic super-eruptions. *Geophys. Res. Lett.* **37**, n/a–n/a (2010).
- Osipov, S., Stenchikov, G., Tsigaridis, K., LeGrande, A. N. & Bauer, S. E. The role of the SO<sub>2</sub> radiative effect in sustaining the volcanic winter and soothing the toba impact on climate. *J. Geophys. Res. Atmos.* **125** <https://doi.org/10.1029/2019JD031726> (2020).
- Ambrose, S. H. Late Pleistocene human population bottlenecks, volcanic winter, and differentiation of modern humans. *J. Hum. Evol.* **34**, 623–651 (1998).
- Rampino, M. & H. Ambrose, S. Volcanic winter in the Garden of Eden: The Toba supereruption and the late Pleistocene human population crash. *Sp. Pap. Geol. Soc. Am.* **345**, 71–82 (2000).
- Malaspinas, A. S. et al. A genomic history of Aboriginal Australia <https://www.nature.com/articles/nature18299> (2016).
- Mallick, S. et al. The Simons Genome Diversity Project: 300 genomes from 142 diverse populations. *Nature* **538**, 201–206 (2016).
- Karmin, M. et al. A recent bottleneck of Y chromosome diversity coincides with a global change in culture. *Genome Res.* **25**, 459–466 (2015).
- Li, H. & Durbin, R. Inference of human population history from individual whole-genome sequences. *Nature* **475**, 493–496 (2011).
- Yost, C. L., Jackson, L. J., Stone, J. R. & Cohen, A. S. Subdecadal phytolith and charcoal records from Lake Malawi, East Africa imply minimal effects on human evolution from the 74 ka Toba supereruption. *J. Hum. Evol.* **116**, 75–94 (2018).
- Chesner, C. A. & Luhr, J. F. A melt inclusion study of the Toba Tuffs, Sumatra, Indonesia. *J. Volcanol. Geotherm. Res.* **197**, 259–278 (2010).
- Brenna, H., Kutterolf, S., Mills, M. J. & Krüger, K. The potential impacts of a sulfur- and halogen-rich supereruption such as Los Chocoyos on the atmosphere and climate. *Atmos. Chem. Phys.* **20**, 6521–6539 (2020).
- Brenna, H., Kutterolf, S. & Krüger, K. Global ozone depletion and increase of UV radiation caused by pre-industrial tropical volcanic eruptions. *Sci. Rep.* **9**, 9435 (2019).
- Wallace, P. J. From mantle to atmosphere: magma degassing, explosive eruptions, and volcanic volatile budgets. *Dev. Volcanol.* **5**, 105–127 (2003).
- Wallace, P. J., Cam, S. A., Rose, W. I., Bluth, G. J. & Gerlach, T. Integrating petrologic and remote sensing perspectives on magmatic volatiles and volcanic degassing. *Eos, Trans. Am. Geophys. Union* **84**, 441 (2011).

25. Wallace, P. J. & Gerlach, T. M. Magmatic vapor source for sulfur dioxide released during volcanic eruptions: evidence from Mount Pinatubo. *Science* **265**, 497–499 (1994).
26. Wallace, P. J. & Edmonds, M. The sulfur budget in magmas: evidence from melt inclusions, submarine glasses, and volcanic gas emissions. *Rev. Mineral Geochem.* **73**, 215–246 (2011).
27. Zielinski, G. A. et al. Potential atmospheric impact of the Toba mega-eruption 71,000 years ago. *Geophys. Res. Lett.* **23**, 837–840 (1996).
28. Traversi, R. et al. Sulfate spikes in the deep layers of EPICA-dome C ice core: evidence of glaciological artifacts. *Environ. Sci. Technol.* **43**, 8737–8743 (2009).
29. Song, S. R. et al. Newly discovered eastern dispersal of the youngest Toba Tuff. *Mar. Geol.* **167**, 303–312 (2000).
30. Huang, C.-Y., Zhao, M., Wang, C.-C. & Wei, G. Cooling of the South China Sea by the Toba Eruption and correlation with other climate proxies 71,000 years ago. *Geophys. Res. Lett.* **28**, 3915–3918 (2001).
31. Timmreck, C. et al. Climate response to the Toba super-eruption: regional changes. *Quaternary Int.* **258**, 30–44 (2012).
32. Stoffel, M. et al. Estimates of volcanic-induced cooling in the Northern Hemisphere over the past 1,500 years. *Nat. Geosci.* **8**, 784–788 (2015).
33. Lane, C. S., Chorn, B. T. & Johnson, T. C. Ash from the Toba supereruption in Lake Malawi shows no volcanic winter in East Africa at 75 ka. *Proc. Natl Acad. Sci. USA* (2013). <http://www.pnas.org/content/early/2013/04/24/1301474110.abstract>.
34. Mills, M. J., Toon, O. B., Turco, R. P., Kinnison, D. E. & Garcia, R. R. Massive global ozone loss predicted following regional nuclear conflict. *Proc. Natl Acad. Sci. USA* **105**, 5307–5312 (2008).
35. Mills, M. J., Toon, O. B., Lee-Taylor, J. & Robock, A. Multidecadal global cooling and unprecedented ozone loss following a regional nuclear conflict. *Earth's Future* **2**, 161–176 (2014).
36. Solomon, S. Stratospheric ozone depletion: a review of concepts and history. *Rev. Geophys.* **37**, 275–316 (1999).
37. Textor, C., Graf, H.-F., Timmreck, C. & Robock, A. Emissions from volcanoes. 269–303 (2004).
38. Wade, D. C. et al. Reconciling the climate and ozone response to the 1257 CE Mount Samalas eruption. *Proc. Natl Acad. Sci. USA* **117**, 26651–26659 (2020).
39. Bekki, S., Toumi, R. & Pyle, J. A. Role of sulphur photochemistry in tropical ozone changes after the eruption of Mount Pinatubo. *Nature* **362**, 331–333 (1993).
40. Michelangeli, D. V., Allen, M. & Yung, Y. L. El Chichon volcanic aerosols: impact of radiative, thermal, and chemical perturbations. *J. Geophys. Res.* **94**, 18429–18443 (1989).
41. Bekki, S. et al. The role of microphysical and chemical processes in prolonging the climate forcing of the Toba Eruption. *Geophys. Res. Lett.* **23**, 2669–2672 (1996).
42. Bekki, S. Oxidation of volcanic SO<sub>2</sub>: a sink for stratospheric OH and H<sub>2</sub>O. *Geophys. Res. Lett.* **22**, 913–916 (1995).
43. van der Leun, J. C., Tang, X. & Tevini, M. Environmental effects of ozone depletion: 1998 assessment (1998).
44. Björn, L. O. & McKenzie, R. L. Ozone depletion and the effects of ultraviolet radiation. In *Photobiology: The Science of Life and Light: Second Edition*, 503–530 (Springer New York, 2008).
45. Eric Klobas, J., Wilmouth, D. M., Weisenstein, D. K., Anderson, J. G. & Salawitch, R. J. Ozone depletion following future volcanic eruptions. *Geophys. Res. Lett.* **44**, 7490–7499 (2017).
46. Cadoux, A., Scaillet, B., Bekki, S., Oppenheimer, C. & Druitt, T. H. Stratospheric Ozone destruction by the Bronze-Age Minoan eruption (Santorini Volcano, Greece). *Sci. Rep.* **5**, 12243 (2015).
47. Black, B. A., Lamarque, J. F., Shields, C. A., Elkins-Tanton, L. T. & Kiehl, J. T. Acid rain and ozone depletion from pulsed siberian traps magmatism. *Geology* **42**, 67–70 (2014).
48. Benca, J. P., Duijnste, I. A. & Looy, C. V. UV-B-induced forest sterility: Implications of ozone shield failure in earth's largest extinction. *Sci. Adv.* **4**, e1700618 (2018).
49. Schmidt, G. A. et al. Present-day atmospheric simulations using GISS Model E: comparison to In Situ, satellite, and reanalysis data. *J. Clim.* **19**, 153–192 (2006).
50. Shindell, D. T. et al. Interactive ozone and methane chemistry in GISS-E2 historical and future climate simulations. *Atmos. Chem. Phys.* **13**, 2653–2689 (2013).
51. Koch, D., Schmidt, G. A. & Field, C. V. Sulfur, sea salt, and radionuclide aerosols in GISS Model E. *J. Geophys. Res. Atmos.* **111** <https://doi.org/10.1029/2004JD005550> (2006).
52. Koch, D., Jacob, D., Tegen, I., Rind, D. & Chin, M. Tropospheric sulfur simulation and sulfate direct radiative forcing in the Goddard Institute for Space Studies general circulation model. *J. Geophys. Res. Atmos.* **104**, 23799–23822 (1999).
53. Guo, S., Bluth, G. J. S., Rose, W. I., Watson, I. M. & Prata, A. J. Re-evaluation of SO<sub>2</sub> release of the 15 June 1991 Pinatubo eruption using ultraviolet and infrared satellite sensors. *Geochem. Geophys. Geosyst.* **5** <https://doi.org/10.1029/2003GC000654> (2004).
54. Wild, O., Zhu, X. & Prather, M. J. Fast-J: accurate simulation of in- and below-cloud photolysis in tropospheric chemical models. *J. Atmos. Chem.* **37**, 245–282 (2000).
55. Bianz, H. & Prather, M. J. Fast-J2: accurate simulation of stratospheric photolysis in global chemical models. *J. Atmos. Chem.* **41**, 281–296 (2002).
56. Madronich, S. & Flocke, S. Theoretical estimation of biologically effective UV radiation at the earth's surface. In *Solar Ultraviolet Radiation*, 23–48 (Springer Berlin Heidelberg, 1997). [https://doi.org/10.1007/978-3-662-03375-3\\_3](https://doi.org/10.1007/978-3-662-03375-3_3).
57. A.F. McKinlay, A. & Diffey, B. A reference action spectrum for ultraviolet-induced erythema in human skin. In *Human Exposure to Ultraviolet Radiation: Risks and Regulations*, 83–87 (1987).
58. Gelaro, R. et al. The modern-era retrospective analysis for research and applications, version 2 (MERRA-2). *J. Clim.* **30**, 5419–5454 (2017).

### Acknowledgements

We thank Albrecht W. Hofmann for his help with the interpretation of melt inclusion data. The research was supported by funding from King Abdullah University of Science and Technology (KAUST), NASA ACMAP (Atmospheric Composition Modeling and Analysis Program) Contract NNX15AE36G, and International Scientific Partnership Program (ISPP) of the King Saud University.

### Author contributions

S.O. conducted the model simulations and analyzed the results. S.O. and J.L. drafted the article. J.L., G.S., and M.F. contributed to the analyses, and K.T., A.L., and S.B. to model development. All authors contributed to writing of the article.

### Funding

Open Access funding enabled and organized by Projekt DEAL.

### Competing interests

The authors declare that they have no competing interests.

### Additional information

**Supplementary information** The online version contains supplementary material available at <https://doi.org/10.1038/s43247-021-00141-7>.

**Correspondence** and requests for materials should be addressed to S.O.

**Peer review information** Primary handling editor: Emma Liu, Joe Aslin

**Reprints and permission information** is available at <http://www.nature.com/reprints>

**Publisher's note** Springer Nature remains neutral with regard to jurisdictional claims in published maps and institutional affiliations.



**Open Access** This article is licensed under a Creative Commons

Attribution 4.0 International License, which permits use, sharing, adaptation, distribution and reproduction in any medium or format, as long as you give appropriate credit to the original author(s) and the source, provide a link to the Creative Commons license, and indicate if changes were made. The images or other third party material in this article are included in the article's Creative Commons license, unless indicated otherwise in a credit line to the material. If material is not included in the article's Creative Commons license and your intended use is not permitted by statutory regulation or exceeds the permitted use, you will need to obtain permission directly from the copyright holder. To view a copy of this license, visit <http://creativecommons.org/licenses/by/4.0/>.

© The Author(s) 2021